ACCOUNTS
of chemical research

Something from Nothing: Enhancing Electrochemical Charge Storage with Cation Vacancies

BENJAMIN P. HAHN, JEFFREY W. LONG,*
AND DEBRA R. ROLISON*

Surface Chemistry Branch (Code 6170), U.S. Naval Research Laboratory, Washington, D.C. 20375, United States

RECEIVED ON SEPTEMBER 15, 2011

CONSPECTUS

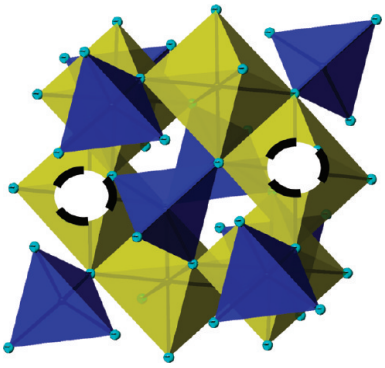

The performance of electrochemical energy storage devices (e.g., batteries and electrochemical capacitors) is largely determined by the physicochemical properties of the active electrode materials, such as the thermodynamic potential associated with the charge-storage reaction, ion-storage capacity, and long-term electrochemical stability. In the case of mixed ion/electron-conducting metal oxides that undergo cation-insertion reactions, the presence of cation vacancies in the lattice structure can enhance one or more of these technical parameters without resorting to a drastic change in material composition. Examples of this enhancement include the charge-storage properties of certain cation-deficient oxides such as γ-MnO_2 and γ-Fe_2O_3 relative to their defect-free analogues. The optimal cation-vacancy fraction is both material- and application-dependent because cation vacancies enhance some materials properties at the expense of others, potentially affecting electronic conductivity or thermal stability. Although the advantages of structural cation vacancies have been known since at least the mid-1980s, only a handful of research groups have purposefully integrated cation vacancies into active electrode materials to enhance device performance.

Three protocols are available for the incorporation of cation vacancies into transition metal oxides to improve performance in both aqueous and nonaqueous energy storage. Through a processing approach, researchers induce point defects in conventional oxides using traditional solid-state-ionics techniques that treat the oxide under appropriate atmospheric conditions with a driving force such as temperature. In a synthetic approach, substitutional doping of a highly oxidized cation into a metal-oxide framework can significantly increase cation-vacancy content and corresponding charge-storage capacity. In a scaling approach, electrode materials that are expressed in morphologies with high surface areas, such as aerogels, contain more defects because the increased fraction of surface sites favors the formation of cation vacancies.

In this Account, we review studies of cation-deficient electrode materials from the literature and our laboratory, focusing on transition metal oxides and the impact cation vacancies have on electrochemical performance. We also discuss the challenges and limitations of these defective structures and their promise as battery materials.

Introduction

Electrochemical energy storage underpins the development of advanced power sources in support of technologies ranging from portable consumer electronics to transportation to grid-scale applications.[1] The performance of such energy-storage devices as batteries and electrochemical capacitors is largely determined by the properties of the active electrode materials, which, in turn, are influenced by a number of physicochemical properties (e.g., composition, structure, morphology). Expressing electrode materials in nanoscale and architectured forms is a common approach to improve high rate performance,[1,2] while particular crystal phases (e.g., spinel and olivine) are more favorable for cation-insertion charge-storage mechanisms.[3] One underutilized design strategy to increase capacity and improve ion-insertion potential is to deliberately incorporate cation

Published on the Web 05/29/2012 www.pubs.acs.org/accounts
10.1021/ar200238w

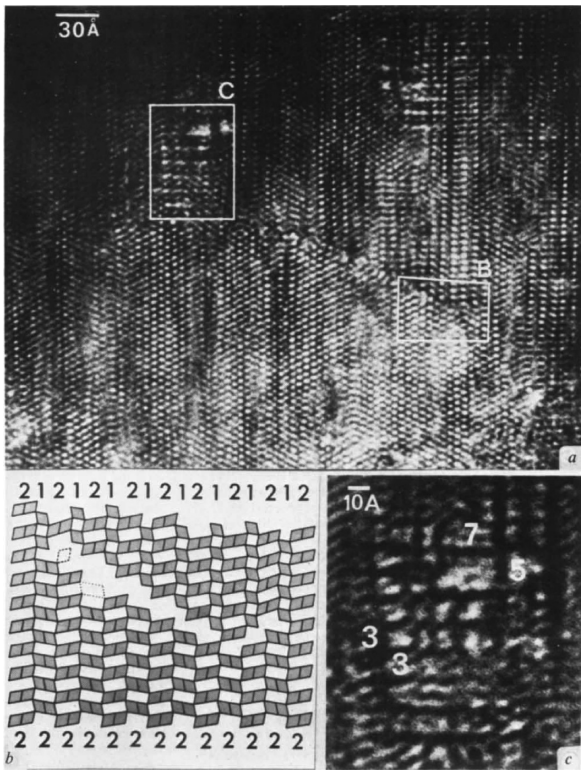

FIGURE 1. Defects in nsutite mineral ore (Piedras Negras, Mexico): (a) high-resolution TEM image; (b) cartoon of proposed lattice structure in box B; (c) enlargement of box C illustrating multiple tunnel-like defects. Atomic structure in box C is consistent with todorokite inclusion. Reprinted with permission from ref 4. Copyright 1983 Macmillan Publishers Ltd.

vacancies into the lattice structure of the insertion oxide, which in many respects offers something (extra energy storage) for nothing (the absence of the metal ion in its lattice site).

Naturally occurring cation-deficient metal oxides (e.g., maghemite, nsutite) have been known in the mineralogy community for decades, but the first comprehensive studies to correlate structural vacancies with charge-storage properties were not published until the mid-1980s. At that time, Turner and Buseck[4] observed vacancy clustering in nsutite, γ-MnO_2, by high-resolution transmission electron microscopy (Figure 1) and proposed that these defects influence proton-transport properties. Subsequently, Ruetschi[5−7] formulated a cation-vacancy model that explained why some phases of MnO_2 are more electrochemically active than others when used as positive electrode materials for primary alkaline cells. In maghemite (γ-Fe_2O_3 or rather, $Fe^{3+}_{2.67}\square_{0.33}O_4$), Chabre and co-workers[8] electrochemically inserted Li^+ from nonaqueous electrolytes into octahedral Fe^{2+} vacancies at potentials that precede the irreversible phase transformation of the spinel habit to rocksalt. These reports laid the groundwork for further exploration into the charge-storage properties of cation-deficient electrode materials and their potential use for commercial energy-storage applications.

The cation-vacancy content in certain first-row transition metal oxides (e.g., Fe, Mn, V) can be tailored through modified synthetic procedures, such as replacing a fraction of the native metal cations with a more highly oxidized substituent,[9,10] treating stoichiometric oxides at temperature in defect-inducing atmospheres,[11] and expressing the oxide as a nanomaterial with a high surface-to-volume ratio to amplify surface defects.[12] Elucidating the presence and distribution of cation vacancies in the host structure is usually challenging, particularly for materials that are nanoscopic or poorly crystalline, and multiple analytical techniques, including spectroscopy (such as infrared, Raman scattering, nuclear magnetic resonance, and X-ray absorption), X-ray diffraction (XRD), and high-resolution transmission electron microscopy (HRTEM), are often necessary to understand the physical nature of such materials. Not surprisingly, the presence of cation vacancies and their influence on electrochemical properties is still a subject of debate. Herein we describe particular examples of cation-deficient metal oxides and their corresponding electrochemical properties, ranging from the well-characterized electrolytic MnO_2 for proton insertion in alkaline electrolytes to more speculative cases such as aerogel-like forms of V_2O_5 for Li-ion insertion in nonaqueous electrolytes.

Overview of Cation-Deficient Materials

Manganese Oxide. Manganese oxides are extensively used for electrochemical charge storage, typically as a positive electrode material, in configurations ranging from the ubiquitous Zn/MnO_2 alkaline battery[13] to rechargeable Li-ion batteries[14] and more recently in asymmetric electrochemical capacitors.[15] Manganese oxides exhibit a diverse range of compositions and polymorphs, some of which exhibit defects and vacancies that are critical to their performance as electrode materials. For example, the γ- and ε-MnO_2 phases have long been used as the active positive electrode material for Zn/MnO_2 alkaline cells, but it was not until the 1980s that Ruetschi recognized the importance of cation vacancies for the proton-insertion properties of these particular intergrowths of MnO_2 (Figure 2a).[5,6] Electrolytic γ- and ε-MnO_2 both contain structural Mn^{4+} vacancies with charge neutrality maintained by four protons present in the lattice as OH^- for each Mn^{4+} vacancy. These proton-compensated vacancies enhance the thermodynamic reactivity of the oxide by lowering the activation energy needed

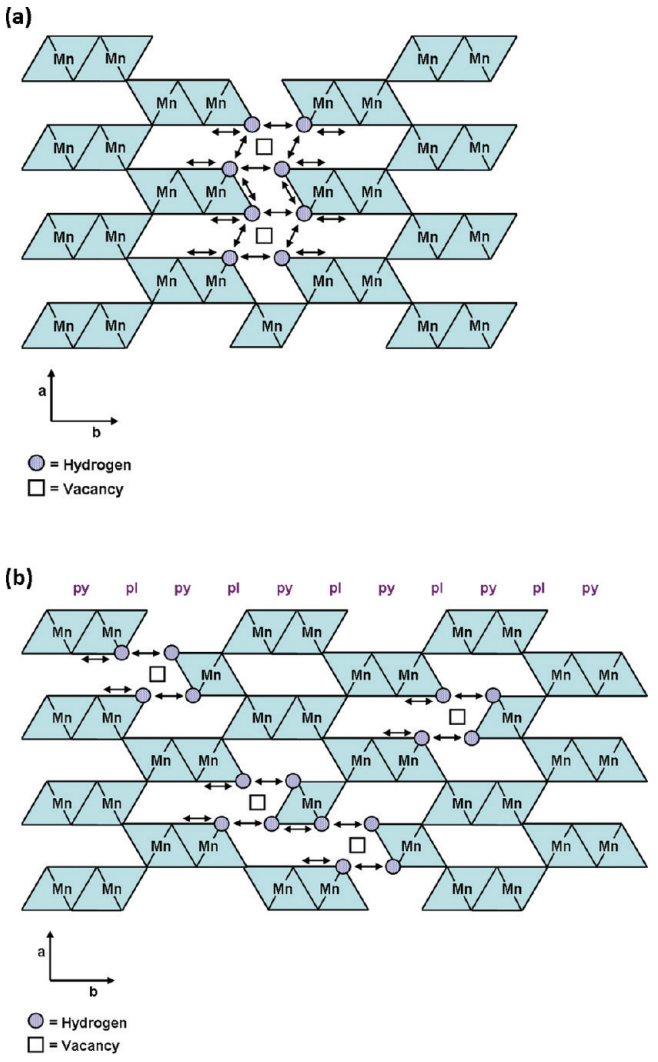

FIGURE 2. Cartoons of cation-deficient MnO_2 phases viewed along the [001] direction illustrating two different defect configurations: (a) γ-MnO_2 intergrowth structure with chain-like vacancy clustering and (b) R-MnO_2 with point defects. Arrows depict some possible proton-transport pathways associated with cation-vacant sites. Reproduced with permission from ref 7. Copyright 1988 The Electrochemical Society.

to shuttle protons throughout the lattice.[7] The direct relationship between the proton and vacancy content in electrolytic MnO_2 allowed Ruetschi to estimate the vacancy fraction through standard materials characterization techniques (i.e., pycnometry, thermogravimetry) and subsequently correlate the cation-vacancy content to electrochemical performance metrics in aqueous media (i.e., proton-transfer rate, electrode potential).

Because cation-deficient MnO_2 phases cannot be fully dehydrated thermally without healing out the structural cation vacancies, it is pertinent to consider how protons and water within the lattice influence electrochemical charge storage. In the Ruetschi cation-vacancy model, protons associated with MnO_2 phases are categorized as either (1) localized "Ruetschi" protons that charge-compensate Mn^{4+} vacancies or (2) mobile "Coleman" protons that associate with Mn^{3+} during reduction. The quantity of Ruetschi protons in defective MnO_2 phases affects the number of Coleman protons that can be inserted electrochemically, where the theoretical capacity is lowered as the proton/water content increases.[5]

By definition, Ruetschi protons are statistically immobile (i.e., there are always four protons per Mn^{4+} vacancy) but can hypothetically move to adjacent electron-donating sites (e.g., O^{2-}) when replaced by other protons. This vacancy-related mechanism for proton exchange facilitates electrochemical insertion/extraction at higher rates in defective MnO_2 phases and is the prevalent theory in the literature for describing how cation-deficient materials achieve enhanced rate capability in aqueous solution. Ruetschi protons also make proton insertion into MnO_2 more thermodynamically favorable, raising the electrode potential in a predictable fashion, due to the lower electrostatic repulsion at vacancy sites relative to Mn^{4+} sites.[6,16] As a result, the electrochemical insertion of electrolyte cations is more energetically favorable near proton-compensated vacancies than near Mn^{4+} cations, and the EMF for ion-insertion shifts positive as more proton-compensated vacancies are incorporated into the lattice, thereby increasing the voltage of the cell.

Unfortunately, the large variety of polymorphs and defect structures within the MnO_2 phase space complicates literature comparisons of cation-deficient MnO_2 materials. For example, cation-deficient γ-MnO_2 has an intergrowth structure where pyrolusite (β-MnO_2) channels exist within a ramsdellite (R-MnO_2) framework;[17] in addition to cation vacancies, the γ-MnO_2 phase can assume varying degrees of pyrolusite domains (P_r) and microtwinning defects (T_w).[13] Not surprisingly, the P_r and T_w fractions are reported to influence the charge-storage mechanism.[18] The γ-MnO_2 structure has been attributed to electrolytic manganese dioxide (EMD) materials used in primary alkaline batteries for years, but recently Heuer and co-workers[19] suggested that EMD is at least partially comprised of the cation-deficient ε-phase and that the γ-MnO_2 label does not accurately describe commercial EMD. The inconsistency exhibited in the published results detailing the electrochemical properties of defect MnO_2 phases likely arises from subtle differences in the active electrode material, where the cation vacancy content is only one of several physical parameters that impacts electrochemical performance.

According to Ruetschi and Giovanoli,[7] proton conduction becomes enhanced along one or more crystallographic planes depending upon how the defects are arranged. The possible configurations for proton-compensated cation vacancies as defined within the MnO_2 lattice are chain-like clusters (Figure 2a), organized point defects (Figure 2b), or surface defects. In the model point-defective R-MnO_2 structure, proton transport typically occurs preferentially along the pyramidal oxygen sites (as seen by projecting onto the (001) plane where Ruetschi protons are situated near isolated Mn^{4+} octahedral vacancies, Figure 2b).[20,21] With proton-compensated vacancies present, inserting protons can also be redirected to planar oxygen sites.[7]

Chain-like clustering, as depicted in the intergrowth structure in Figure 2a, has been observed in γ-MnO_2 by HRTEM;[4] depending on the lattice structure, such formations may enhance proton conduction along the axis of the vacancy cluster via proton-transport bridges.[7] Finally, the surface layer of MnO_2 contains defects even under ambient conditions; in a sufficiently humid environment, oxygen sites can bind protons through hydroxylation causing the formation of a "virtual layer" of cation vacancies as terminating surface hydroxyls. Studies by Donne and co-workers[22] suggest that only basic surface hydroxyl groups actively facilitate proton insertion.

Although the electrochemical properties of cation-deficient MnO_2 phases can vary significantly with the defect structure of the active electrode material and the cell conditions (e.g., pH, electrolyte, etc.), some general statements can be made concerning the proton-insertion mechanism. Ignoring for the moment the surface reactions that influence electrochemical charge storage, cation-deficient MnO_2 reversibly injects $\sim 0.5H^+$ per formula unit over many cycles at slow discharge rates (e.g., $\sim$10 mA g^{-1}, for a *C*/30 rate, where a 1*C* rate is full discharge of the battery capacity in 1 h).[13,23] Proton insertion initially leads to the formation of a more disordered groutellite (MnOOH)-based system; as the ion-insertion capacity increases, Jahn–Teller distortion occurs in conjunction with generation of Mn^{3+}, which forms strong hydrogen bonds causing an irreversible structural transformation to groutite (α-MnOOH).[13]

Ion-insertion/extraction limitations associated with the ramsdellite→groutite transition may be less apparent in highly disordered MnO_2 compositions, especially those with a high degree of microtwinning that disrupts the structural transition leading to Jahn–Teller propagation.[13] Unfortunately, parasitic side reactions involving Mn^{3+} in alkaline media further complicate the charge-storage mechanism.[13] As the discharge potential is pushed further negative, Mn^{3+} disproportionates to Mn^{4+} and Mn^{2+}; the divalent ion forms complex ions in solution that drive precipitation of manganese hydroxide.[24]

Cation-deficient MnO_2 has also been investigated as a Li^+-insertion host in nonaqueous electrolytes for rechargeable Li batteries. To reduce the possibility of gas generation (e.g., H_2, CO_2) during electrochemical cycling, MnO_2 is often thermally treated to remove the associated protons and structural H_2O. Researchers typically dehydrate cation-deficient γ-MnO_2 by sintering the composition to 250–400 °C to form a structural derivative referred to as heat-treated manganese dioxide (HTMD) or heat-treated electrolytic manganese dioxide (HEMD); however, the defect structure and electrochemical performance of HTMD/HEMD materials can vary significantly from one product to the next depending upon the physicochemical properties and intergrowth character of the γ-MnO_2 precursor.[25] During calcination to form HTMD, γ-MnO_2 becomes more β-like in nature as defects are removed.[26]

Although Ruetschi previously demonstrated methods to estimate the cation-vacancy content in electrolytic MnO_2 after sintering, it is not clear whether any remaining proton-compensated cation vacancies affect the charge-storage mechanism for Li^+ insertion from nonaqueous electrolytes. Optimization studies suggest the reversible Li-ion storage capacity of HTMD is maximized when the lattice character is most similar to pure R-MnO_2; however, HTMD structures resembling β-MnO_2 also perform well if a small fraction of microtwinning defects are present to accommodate the phase transformation that occurs upon electroreduction/cation insertion during electrochemical lithiation.[18] Typical Li^+-insertion capacities for HTMD achieved in the first discharge cycle exceed 200 mA h g^{-1} (between 3.8 and 2.0 V vs Li) at low rates (5–9 mA g^{-1}); but on subsequent cycles, the capacity ranges between 130 and 180 mA h g^{-1}, depending on the particular heat treatment applied to the HTMD.[27]

Recently, Jung et al. proposed an alternative to HTMD by dehydrating electrolytic γ-MnO_2 through nonaqueous chemical oxidation under low partial pressures of oxygen using nitronium tetrafluoroborate (NO_2BF_4); this process removes protons and water while avoiding crystallographic conversion and yields Li-ion discharge capacity approaching 250 mA h g^{-1} over six cycles.[28,29] When chemically oxidized γ-MnO_2 is lithiated with *n*-butyllithium, made into a powder composite electrode, and cycled in a nonaqueous lithium-based electrolyte, the initial charge profile shows two plateaus at approximately 3.1 and 3.6 V vs Li.[29] The authors

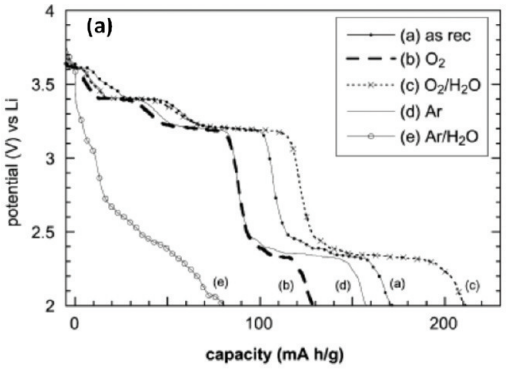

(b)

Treatment of μm-V_2O_5	Capacity (±4%)	% change	Δ in XRD
As-received 1-μm powder	172 mAh g^{-1}	0	N/A
O_2 annealed at 460 °C stoichiometric	129	–25%	no
O_2/H_2O annealed at 460 °C cation vacancies	212	+23%	no
Ar annealed at 460 °C V^{4+}/anion vacancies	158	–8%	no
Ar/H_2O annealed at 460 °C V^{4+}/anion & cation vacancies	72	–58%	yes

FIGURE 3. (a) Galvanostatic discharge curves acquired in 1 M $LiClO_4$/propylene carbonate using V_2O_5 sintered under different atmospheres at 460 °C; applied current density is 20 μA g^{-1}. Reprinted with permission from ref 11. Copyright 2002 Elsevier. (b) Table showing the effect of the temperature/atmosphere treatment on bulk structure and lithium-ion capacity; the only treatment that enhances Li-ion capacity is the one that creates proton-stabilized cation vacancies (i.e., O_2/H_2O).

ascribe the first plateau at 3.1 V to removal of Li^+ from octahedral sites or Mn^{3+} channels, while the second plateau at 3.6 V is attributed to the removal of Li^+ in the vicinity of Mn^{4+} vacancies.[29] What is less clear is how Mn^{4+} vacancies are stabilized when, as the authors state, nitronium-based oxidation removes charge-compensating Ruetschi protons.[29]

Vanadium Oxide. Vanadium oxides were among the earliest candidates to be investigated as positive electrode materials for rechargeable Li batteries. The interest in vanadium oxides, particularly V_2O_5 and V_6O_{13}, continues to the present day as driven by the promise of high capacities approaching or exceeding 300 mA h g^{-1}.[30,31] In the case of V_2O_5, the Li-insertion mechanism is complex with multiple phase transformations possible depending upon the depth of discharge.[32] One such modification, ω-$Li_xV_2O_5$ ($0.4 \leq x \leq 3$), has been reported to deliver a stable Li-insertion capacity of 310 mA h g^{-1} over 30 cycles under low discharge-rate operation (*C*/20).[33] Mixed-valent V_6O_{13} has also been recognized as a possible cathode material for low-voltage batteries, exhibiting insertion capacities as high as six Li per formula unit.[34] Efforts to improve charge-storage properties for such oxide compositions include various nanostructured approaches[35] and deviations from stoichiometry (e.g., V_6O_{13+y}).[36]

Swider-Lyons et al.[11] attempted to incorporate defects within micrometer-sized polycrystalline commercial V_2O_5 powders by using controlled temperature and atmosphere treatments. When temperature and atmosphere conditions were used to create proton-compensated cation vacancies (460 °C under an O_2/H_2O atmosphere), the Li-ion capacity was boosted by 23% relative to the as-received V_2O_5 (Figure 3). Heating in atmospheres that should have removed or created oxygen (anion) vacancies (O_2 and Ar, respectively) or created Schottky defects (paired cation and anion vacancies using Ar/H_2O) resulted in products that had decreased Li-ion capacity relative to the as-received V_2O_5.

The effects demonstrated with microcrystalline forms of cation-deficient V_2O_5 are enhanced further when the oxide is prepared via low-temperature sol–gel routes that lead to ultraporous, high-surface-area aerogels (75–99% void space) and related aerogel-like nanoarchitectures.[37] Because aerogels are inherently "all-surface" materials,[38] the aerogel architecture (Figure 4) is hypothesized to contain a high concentration of structural defects,[39] including proton-compensated cation vacancies.[12] The existence of cation vacancies has not been directly confirmed through high-resolution imaging, but their presence is posited from the exceptional charge-storage properties of aerogel-based electrode materials.[12] For example, under the "classical" charge-storage mechanism, only 2 equiv of Li can be inserted into V_2O_5 (Scheme 1).

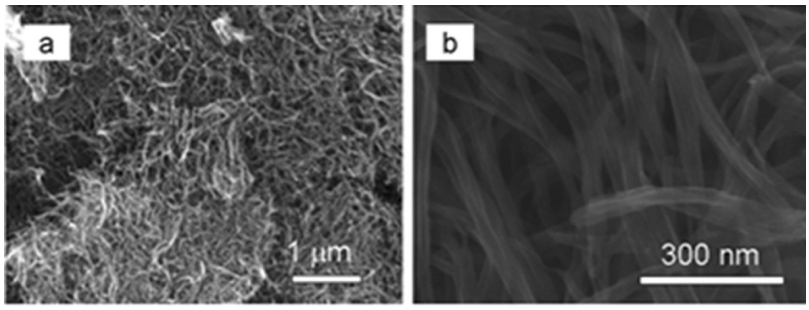

FIGURE 4. Micrographs of $V_2O_5 \cdot xH_2O$ aerogel acquired by scanning electron microscopy at (a) low-resolution and (b) high-resolution. Reprinted with permission from ref 37. Copyright 2011 Royal Society of Chemistry.

SCHEME 1. Li Insertion into V_2O_5 (Written as $VO_{2.5}$)[a]

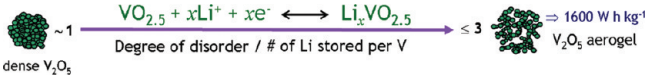

[a]By the "classic" intercalation mechanism, V_2O_5 can accommodate up to one Li per V; however, certain low-density V_2O_5 materials can accommodate up to three Li per V.

Pioneering work exploring the Li-ion-storage properties of V_2O_5 aerogels demonstrated capacities of four Li ions per V_2O_5 unit,[40−42] and a follow-up study reported capacities exceeding five Li ions per V_2O_5 unit as derived via both chemical and electrochemical lithiation processes.[43] Because the classical intercalation reaction cannot adequately describe these experimental observations, it has been concluded that V_2O_5 aerogels also store charge through one or more separate, nonconventional ion-insertion mechanisms.[12] X-ray absorption spectroscopy (XAS) and X-ray photoelectron spectroscopy (XPS) of V_2O_5 aerogels chemically lithiated to varying degrees support the hypothesis that vanadium sites are not reduced during Li-ion insertion, but instead, incoming Li^+ associates with the oxygen sites and delocalizes positive charge over the anion framework.[43] Such a Li-insertion mechanism is plausible but still open to debate; a subsequent XAS report[44] suggested that Li^+ electrochemically inserts into V_2O_5 aerogels through a multivalent reduction process ($V^{5+} \rightarrow V^{4+} \rightarrow V^{3+}$).

The charge-storage properties are agreed to be influenced by several factors, including the interlayer water content,[45] pore structure,[46] degree of crystallinity,[47] and defect concentration.[48] On the basis of our knowledge of cation-deficient MnO_2, the existence of proton-compensated cation vacancies within V_2O_5 aerogels is supported by evidence of structural water within the material[40] and electrochemical charge-storage studies that show enhanced rate capability[49] and large insertion capacities.[40,42,43] Furthermore, the high degree of disorder and short diffusion distances permit the reversible insertion of polyvalent cations (e.g., Mg^{2+}) and cations with an ionic radius significantly larger than Li^+ (e.g., K^+, Ba^{2+}).[50]

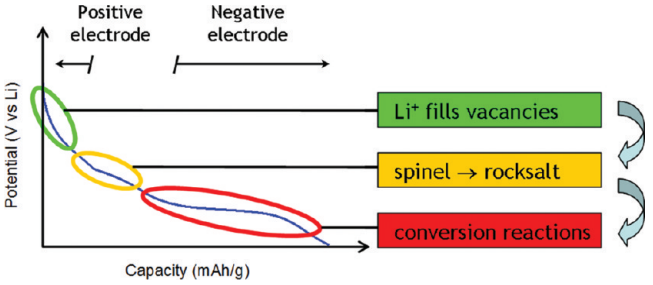

FIGURE 5. Cartoon illustrating the general electrochemical lithiation process for cation-deficient spinel ferrites, proceeding from ion-insertion into cation-vacant sites to the irreversible formation of the rocksalt structure to conversion reactions at deep discharge.

Iron Oxide. Several iron oxide phases have been examined as electrode materials, with particular interest in conversion-type reactions at deep discharge (at potentials <1.4 V vs Li) for use as negative electrodes in Li-ion batteries, but the middling thermodynamic insertion potential associated with the $Fe^{2+/3+}$ redox couple limits the application of iron oxides as positive electrodes (Figure 5).[14,51] However, spinel ferrites with the Fe_3O_4/γ-Fe_2O_3 structure provide another important example of the influence cation vacancies can assert on electrochemical charge storage. Maghemite (γ-Fe_2O_3 or $Fe^{3+}_{2.67}\square_{0.33}O_4$) is the cation-deficient form of Fe_3O_4 in which cation vacancies form to compensate for the oxidation of Fe^{2+} to Fe^{3+}. Pernet et al.[8] explored the Li-insertion mechanism for microcrystalline γ-Fe_2O_3 through chemical and electrochemical lithiation procedures and determined that cation vacancies accommodate ~0.25 mol of Li per formula unit prior to the irreversible spinel-to-rocksalt transformation that occurs during deep discharge (Figure 6). Although this finding does not qualify γ-Fe_2O_3 as a practical positive electrode material for lithium batteries, it does suggest that the cation-deficient γ-Fe_2O_3 structure

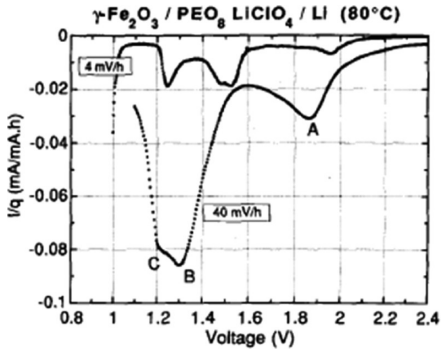

FIGURE 6. Slow linear-sweep voltammograms of $Li_xFe_2O_3$ immersed in a $LiClO_4$/poly(ethylene oxide) (PEO) electrolyte at 80 °C. Peak labels A, B, and C denote different electrochemical lithiation reactions where A correlates with Li-ion insertion into cation vacancies. Voltage is referenced to Li. Reprinted with permission from ref 8. Copyright 1993 Elsevier.

could serve as a platform for designing more enhanced electrode materials that are both inexpensive and environmentally benign. To this end, Koo et al.[52] recently prepared hollow γ-Fe_2O_3 nanoparticles where cation vacancies occupied 44% of the available iron sites. When used as positive electrode materials in Li coin cells, Li-ion storage capacities were obtained (>200 mA h g^{-1} at a 30 mA g^{-1} rate between 4.5−1.5 V vs Li) with no major structural transformations observed over repeated charge−discharge cycling.

Other efforts to improve the charge-storage capacity of γ-Fe_2O_3 have focused primarily on strategies to reduce the particle size, modify the surface with conducting polymers, and use the material as the negative rather than the positive electrode. Studies by Campet and co-workers[53] show that nanocrystalline γ-Fe_2O_3 (8−10 nm particles) can achieve reversible Li-ion storage capacities >200 mA h g^{-1} between 4.3 and 1.3 V vs Li (conditions that go below the typical potential range of a positive electrode material). Ex-situ XRD experiments suggest that the irreversible spinel-to-rocksalt transition that occurs during Li insertion (at $x \approx 0.86$)[8] is suppressed by shrinking the particle size,[54] implying that large, reversible (or at least quasi-reversible) capacities can be achieved at low potentials (from 2 V down to 1 V vs Li). Incorporating γ-Fe_2O_3 nanoparticles in a composite with poly(pyrroles) also improves the reversible Li-insertion capacity by enhancing the kinetics of the electrochemical insertion/extraction process.[55]

While these accomplishments are noteworthy, we find that the charge-storage capacity of γ-Fe_2O_3 and related materials, when used at potentials of relevance for a positive electrode, can be enhanced even further by increasing the concentration of cation vacancies while maintaining the spinel structure. Synthetic approaches for increasing the cation vacancy fraction are not complicated, as described for prototype materials below.

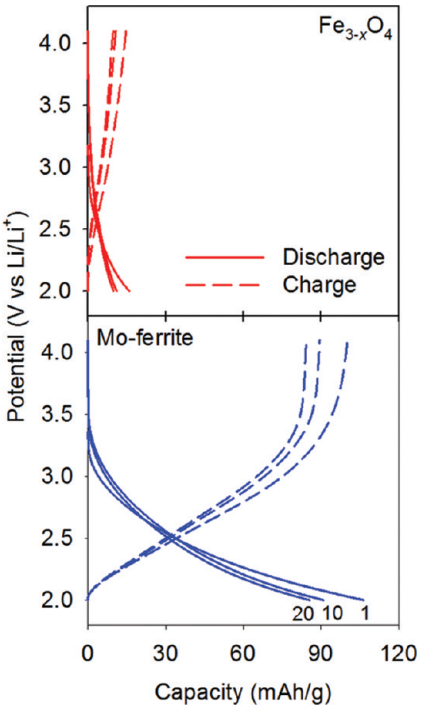

FIGURE 7. Galvanostatic Li-ion charge-storage studies comparing the electrochemical properties of $Mo^{6+}_{0.59}Fe^{3+}_{1.50}\square_{0.91}O_4 \cdot nH_2O$ (Mo-ferrite) versus the parent oxide ($Fe_{3-x}O_4$) in 1 M $LiClO_4$/propylene carbonate. Cycles 1, 10, and 20 are shown; applied current is 20 mA g^{-1}. Reprinted with permission from ref 10. Copyright 2011 Royal Society of Chemistry.

Induced Vacancy Formation: The Influence of Substituent Cations

One approach to increase the vacancy concentration in metal oxides is to substitute a fraction of the native metal cations in the lattice with more highly oxidized cations, but without restructuring the crystal habit. For example, Gillot and co-workers[56,57] increased the vacancy content in γ-Fe_2O_3 by a factor of 2−3 after substituting a fraction of the Fe^{3+} content with Mo^{6+} and V^{5+} using an aqueous, base-catalyzed precipitation followed by controlled temperature/atmosphere treatments. We explored the Li-insertion/extraction behavior of nanometric forms of base-precipitated γ-Fe_2O_3 and a Mo-substituted relative (Mo-ferrite; proposed formula $Mo^{6+}_{0.59}Fe^{3+}_{1.50}\square_{0.91}O_4 \cdot nH_2O$). The Mo-ferrite demonstrated Li-insertion capacities in excess of 85 mA h g^{-1} between 4.1 and 2.0 V vs Li after 20 cycles in a conventional nonaqueous electrolyte, while the synthetic control ($Fe_{3-x}O_4$) yielded <20 mA h g^{-1} (Figure 7).[10] Although the Li-insertion capacity of Mo-substituted ferrite is not equivalent to commercial electrode materials (e.g., $LiCoO_2$), the reported capacity is high for an electrode material consisting primarily of iron oxide, suggesting that compositions previously thought to be inert can now be tailored for energy-storage relevance by deliberately incorporating cation vacancies into the lattice structure.

Similar performance improvements have been reported for other substituted cation-deficient spinels. Bach et al.[58] explored $Mn_{2.2}Co_{0.27}\square_{0.53}O_4$ as a proton-insertion host in alkaline solution; compared to conventional manganese oxide electrode materials (i.e., γ-MnO_2, $LiMn_2O_4$), the substituted spinel structure demonstrates larger reversible capacities and better rate capability. A related material, $Mn_{2.15}Co_{0.37}\square_{0.48}O_4$, reversibly inserts Li^+ in nonaqueous electrolyte at a capacity of ~85 mA h g^{-1} after multiple cycles with 80–90% Coulombic efficiency.[59] Note that the parent oxide structure, Mn_3O_4, has no rechargeability due to a Jahn–Teller distortion that irreversibly degrades the lattice during electrochemical redox; however, the cation-vacant form appears to minimize the Jahn–Teller effect in the discharged product, leading to greater electrochemical stability.[60] Even lithiated metal oxides that contain very small vacancy fractions show enhanced reversibility, such as $Li_{1.02}Ni_{0.15}Mn_{1.75}\square_{0.08}O_4$, which retains 80% of its initial capacity from 3.3 to 2.3 V vs Li over 200 cycles.[61] The high degree of disorder in $Mn_{2.15}Co_{0.37}\square_{0.48}O_4$ also allows for reversible electrochemical insertion of polyvalent Mg^{2+}, a feat not commonly reported for manganese oxide, with the substituted Mn-oxide achieving reversible capacities of ~30 mA h g^{-1} over a potential range of 4.05–2.8 V vs Li.[62]

Few reports exist on the benefits of using substituted cation-deficient oxides as negative electrode materials for electrochemical energy storage, and the role that cation vacancies may play is not well-defined. One negative electrode material of interest is $Li_{1+x}V_{1-x}O_2$,[63] because although the stoichiometric compound ($x = 0$, $LiVO_2$) does not intercalate Li^+, $Li_{1+x}V_{1-x}O_2$ does at ~0.1 V vs Li, due in part to vanadium cation deficiencies that exist within a fraction of the octahedral sites, which in $LiVO_2$ are occupied with Li^+.[64] Cation vacancies may enhance the electrochemical reactivity of other compositions when used as negative electrodes, but conversion reactions may mask the role cation vacancies may play.

Limitations and Challenges

Cation-deficient electrode materials suffer from two major drawbacks that limit their use in electrochemical energy-storage applications: (1) the defect structure is metastable, and (2) as the vacancy content increases, the electronic conductivity decreases. Thermodynamic stability is a major issue, because cation-deficient structures usually only tolerate a limited temperature range (<100 °C is typical) without experiencing some degree of cation-vacancy loss.[7] This thermal sensitivity is especially relevant for ambigels, aerogels, and other high surface area, ultraporous nanoarchitectures

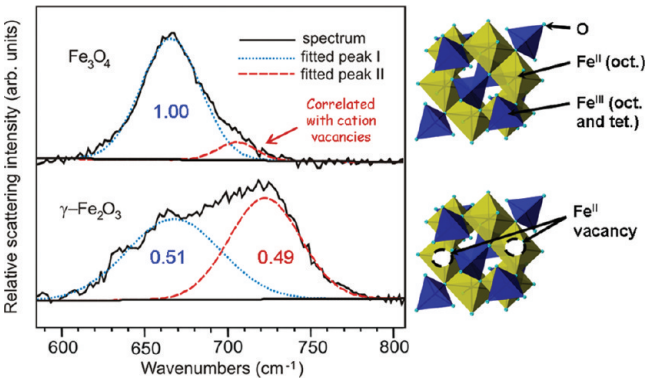

FIGURE 8. Raman spectra from 585–805 cm^{-1} of commercial Fe_3O_4 (top) and γ-Fe_2O_3 (bottom) deconvoluted into low- and high-frequency bands. Reprinted with permission from ref 68. Copyright 2004 American Chemical Society. Cartoons of the respective lattice structures are shown at right.

that may undergo dramatic physical transformations when processed into electrode structures. Surface layers are both highly defective and highly reactive; therefore, other stability issues can arise during electrochemical cycling. For example, structural distortions or irreversible phase transformations that may occur during discharge can permanently decrease the vacancy fraction and concomitantly decrease charge-storage capacity. Just as with defect-free electrode materials, electrochemical stability can sometimes be imposed on metastable materials through creative engineering strategies, such as substitutional doping, tailoring the morphology, or core–shell syntheses with the less-stable phase as the core.[1]

Cation-deficient structures also tend to be less electronically conductive than their defect-free counterparts, because orbital overlap between nearest-neighbor cations provides the pathway for electron conduction. As the cation-vacancy content increases, the average electron-tunneling distance from one cation orbital to another also increases and the electrode material becomes more insulating. In certain defect structures, it is possible to approximate electronic conductivity, σ, based on the vacancy fraction, x, using an exponential relationship between σ and the average electron-tunneling distance, a_t.[5]

Future Opportunities To Make the Most of "Something from Nothing"

Although examples in the literature are still limited in number, sufficient evidence exists to support the promise of cation vacancies to improve cell voltage, capacity, rate capability, and reversibility in batteries and electrochemical capacitors. We see four clear opportunities for future research: (1) current and previously discarded insertion

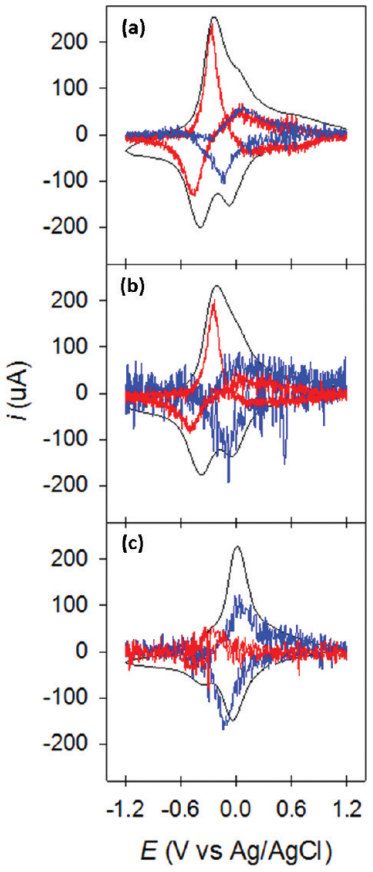

FIGURE 9. Spectroelectrochemical studies of Li-ion insertion and extraction using V_2O_5 sol–gel-derived films on indium–tin oxide (ITO)-coated glass immersed in 1 M $LiClO_4$/propylene carbonate. The voltammetric current (black line) is plotted against the differential absorbance at 400 nm (blue line) and 800 nm (red line). The ITO/vanadia working electrodes were heated to 170 °C under flowing (a) Ar, (b) O_2, and (c) O_2/H_2O atmospheres. Printed with permission from ref 70.

materials need to be re-examined in cation-deficient forms; (2) classic composite electrode structures should be abandoned in favor of advanced electrode architectures; (3) computational efforts are needed to elucidate the electronic structures of cation-deficient insertion materials; (4) synthetic and computational strategies should be developed to stabilize these otherwise metastable phases.

The high vacancy fractions that might otherwise be intriguing to explore in order to push the limits of improved capacity and potential typically diminish the electronic conductivity beyond that practical for use in a conventional powder-composite electrode structure. It may be possible to utilize higher cation vacancy fractions beyond what is classically deemed optimal by moving away from composite electrodes to advanced electrode architectures that allow for more intimate electrical communication between the active material and the electron-conducting phase. Strategies developed to better "wire" electrode materials, such as the thin shell of carbon that coats nanoscale $LiFePO_4$[65] or painting the walls of carbon nanofoam with manganese[66] or iron oxides,[67] will obviate low electron conductivity and allow one to push the limits of cation-vacancy content in charge-insertion nanomaterials.

Subtle differences in crystallography patterns[10] or vibrational spectra[68] (Figure 8) often provide the sole argument for positing that a particular insertion host has cation vacancies, making physical characterization more difficult. Another key challenge is to identify the specific role that structural defects play in the electrochemical charge-storage process. Vanadium oxides are one example where the electronic band structure is known to be influenced by the presence of structural defects from both computation and experiment,[69] an effect that can be exploited for spectroelectrochemical characterization. Rhodes et al.[48,70] investigated the in situ spectroelectrochemical properties of sol–gel-derived V_2O_5 thin films on indium–tin oxide glass substrates and showed that Li-ion-insertion events in the vicinity of anion vacancies (formed by heat treatment in atmospheres with a low partial pressure of O_2) have spectroscopic signatures (centered at a wavelength of 800 nm) distinct from those in stoichiometric V_2O_5 (measured at 400 nm; see Figure 9). Although a useful example of the utility of spectroelectrochemistry, these studies were unable to identify the potential role of cation vacancies, whose spectroscopic signatures are not presently known and may lie in other spectral regions. Further studies of electronic, vibrational, and crystallographic structure using model cation-deficient materials would provide experimentalists with a stronger basis for characterizing and identifying cation vacancies. Without systematic investigations of the electrochemical properties of cation-deficient materials, as expressed in varying arrangements, structures, and compositions, the extent of improvement in electrochemical performance remains uncharted.

We acknowledge the financial support of the U.S. Office of Naval Research.

BIOGRAPHICAL INFORMATION

Benjamin Hahn is a National Research Council Postdoctoral Associate (2009–2012) at the U.S. Naval Research Laboratory (NRL). He received his Ph.D. from the University of Texas at Austin in 2008 and a B.S. from Vanderbilt University in 2004.

Jeffrey Long is a staff scientist in the Surface Chemistry Branch at the NRL where his research centers on the development of nanostructured materials for electrochemical power sources and

separation/filtration. He received a Ph.D. in Chemistry from the University of North Carolina in 1997 and a B.S. from Wake Forest University in 1992.

Debra Rolison heads the Advanced Electrochemical Materials section at the NRL where she and her team design and create multifunctional nanoarchitectures for rate-critical applications, including energy storage and conversion. She received the 2011 ACS Award in the Chemistry of Materials and is a Fellow of the AAAS, MRS, ACS, and AWIS.

FOOTNOTES

*E-mail addresses: jeffrey.long@nrl.navy.mil; rolison@nrl.navy.mil.
The authors declare no competing financial interest.

REFERENCES

1 Rolison, D. R.; Nazar, L. F. Electrochemical energy storage to power the 21st century. *MRS Bull.* **2011**, *36*, 486–493.

2 Rolison, D. R.; Long, J. W.; Lytle, J. C.; Fischer, A. E.; Rhodes, C. P.; McEvoy, T. M.; Bourg, M. E.; Lubers, A. M. Multifunctional 3D nanoarchitectures for energy storage and conversion. *Chem. Soc. Rev.* **2009**, *38*, 226–252.

3 Ohzuku, T.; Brodd, R. J. An overview of positive-electrode materials for advanced lithium-ion batteries. *J. Power Sources* **2007**, *174*, 449–456.

4 Turner, S.; Buseck, P. R. Defects in nsutite (γ-MnO_2) and dry-cell battery efficiency. *Nature* **1983**, *304*, 143–146.

5 Ruetschi, P. Cation-vacancy model for MnO_2. *J. Electrochem. Soc.* **1984**, *131*, 2737–2744.

6 Ruetschi, P. Influence of cation vacancies on the electrode potential of MnO_2. *J. Electrochem. Soc.* **1988**, *135*, 2657–2663.

7 Ruetschi, P.; Giovanoli, R. Cation vacancies in MnO_2 and their influence on electrochemical reactivity. *J. Electrochem. Soc.* **1988**, *135*, 2663–2669.

8 Pernet, M.; Strobel, P.; Bonnet, B.; Bordet, P.; Chabre, Y. Structural and electrochemical study of lithium insertion into γ-Fe_2O_3. *Solid State Ionics* **1993**, *66*, 259–265.

9 Gillot, B.; Domenichini, B.; Tailhades, Ph.; Bouet, L.; Rousset, A. Reactivity of the submicron molybdenum ferrites towards oxygen and formation of new cation deficient spinels. *Solid State Ionics* **1993**, *63*−*65*, 620–627.

10 Hahn, B. P.; Long, J. W.; Mansour, A. N.; Pettigrew, K. A.; Osofsky, M. S.; Rolison, D. R. Electrochemical Li-ion storage in defect spinel iron oxides: The critical role of cation vacancies. *Energy Environ. Sci.* **2011**, *4*, 1495–1502.

11 Swider-Lyons, K. E.; Love, C. T.; Rolison, D. R. Improved lithium capacity of defective V_2O_5 materials. *Solid State Ionics* **2002**, *152*−*153*, 99–104.

12 Rolison, D. R.; Dunn, B. Electrically conductive oxide aerogels: New materials in electrochemistry. *J. Mater. Chem.* **2001**, *11*, 963–980.

13 Chabre, Y.; Pannetier, J. Structural and electrochemical properties of the proton/γ-MnO_2 system. *Prog. Solid State Chem.* **1995**, *23*, 1–130.

14 Thackeray, M. M. Spinel electrodes for lithium batteries. *J. Am. Ceram. Soc.* **1999**, *82*, 3347–3354.

15 Long, J. W.; Bélanger, D.; Brousse, T.; Sugimoto, W.; Sassin, M. B.; Crosnier, O. Asymmetric electrochemical capacitors−Stretching the limits of aqueous electrolytes. *MRS Bull.* **2011**, *36*, 513–522.

16 Balachandran, D.; Morgan, D.; Ceder, G. First principles study of H-insertion in MnO_2. *J. Solid State Chem.* **2002**, *166*, 91–103.

17 De Wolff, P. M. Interpretation of some γ-MnO_2 diffraction patterns. *Acta Crystallogr.* **1959**, *12*, 341–345.

18 Jouanneau, S.; Sarciaux, S.; La Salle, A. L.; Guyomard, D. Influence of structural defects on the insertion behavior of γ-MnO_2: Comparison of H^+ and Li^+. *Solid State Ionics* **2001**, *140*, 223–232.

19 Kim, C.-H.; Akase, Z.; Zhang, L.; Heuer, A. H.; Newman, A. E.; Hughes, P. J. The structure and ordering of ε-MnO_2. *J. Solid State Chem.* **2006**, *179*, 753–774.

20 Maskell, W. C.; Shaw, J. A. E.; Tye, F. L. On the manganese dioxide electrode. V. The evidence indicating the presence of two solid solutions in the range MnO_2−$MnO_{1.5}$ with γ-MnO_2 as one end member. *J. Appl. Electrochem.* **1982**, *12*, 101–108.

21 Maskell, W. C.; Shaw, J. E. A.; Tye, F. L. Manganese dioxide electrode. VIII. Potential vs degree of reduction of oxyhydroxides derived from electrolytic γ-MnO_2: Statistical thermodynamic treatment. *Electrochim. Acta* **1983**, *28*, 225–230.

22 Malloy, A. P.; Browning, G. J.; Donne, S. W. Surface characterization of heat-treated electrolytic manganese dioxide. *J. Colloid Interface Sci.* **2005**, *285*, 653–664.

23 Mondoloni, C.; Laborde, M.; Rioux, J.; Andoni, E.; Lévy-Clément, C. Rechargeable alkaline manganese dioxide batteries I. In situ X-ray diffraction investigation of the H^+/γ-MnO_2 (EMD-type) insertion system. *J. Electrochem. Soc.* **1992**, *139*, 954–959.

24 Kozawa, A.; Yeager, J. F. The cathodic reduction mechanism of electrolytic manganese dioxide in alkaline electrolyte. *J. Electrochem. Soc.* **1965**, *112*, 959–963.

25 Sarciaux, S.; Le Salle, A. L.; Verbaere, A.; Piffard, Y.; Guyomard, D. γ-MnO_2 for Li batteries Part I. γ-MnO_2: Relationships between synthesis conditions, material characteristics and performances in lithium batteries. *J. Power Sources* **1999**, *81*−*82*, 656–660.

26 Paik, Y.; Bowden, W.; Richards, T.; Grey, C. P. The effect of heat-treatment on electrolytic manganese dioxide: A ^2H and ^6Li magic angle spinning NMR study. *J. Electrochem. Soc.* **2005**, *152*, A1539–1547.

27 Ohzuku, T.; Kitagawa, M.; Hirai, T. Electrochemistry of manganese dioxide in lithium nonaqueous cell. II. X-ray diffractional and electrochemical characterization on deep discharge products of electrolytic manganese dioxide. *J. Electrochem. Soc.* **1990**, *137*, 40–46.

28 Jung, W. I.; Sakamoto, K.; Pitteloud, C.; Sonoyama, N.; Yamada, A.; Kanno, R. Chemically oxidized manganese dioxides for lithium secondary batteries. *J. Power Sources* **2007**, *174*, 1137–1141.

29 Jung, W. I.; Nagao, M.; Pitteloud, C.; Itoh, K.; Yamada, A.; Kanno, R. Chemically oxidized γ-MnO_2 for lithium secondary batteries: Structure and intercalation/deintercalation properties. *J. Mater. Chem.* **2009**, *19*, 800–806.

30 Chernova, N. A.; Roppolo, M.; Dillon, A. C.; Whittingham, M. S. Layered vanadium and molybdenum oxides: Batteries and electrochromics. *J. Mater. Chem.* **2009**, *19*, 2526–2552.

31 Höwing, J.; Gustafsson, T.; Thomas, J. O. $Li_{3+\delta}V_6O_{13}$: A short-range-ordered lithium insertion mechanism. *Acta Crystallogr.* **2004**, *B60*, 382–387.

32 Winter, M.; Besenhard, J. O.; Spahr, M. E.; Novák, P. Insertion electrode materials for rechargeable lithium batteries. *Adv. Mater.* **1998**, *10*, 725–763.

33 Leger, C.; Bach, S.; Soudan, P.; Pereira-Ramos, J.-P. Structural and electrochemical properties of ω-$Li_xV_2O_5$ ($0.4 \leq x \leq 3$) as rechargeable cathodic material for lithium batteries. *J. Electrochem. Soc.* **2005**, *152*, A236–A241.

34 Whittingham, M. S. Lithium batteries and cathode materials. *Chem. Rev.* **2004**, *104*, 4271–4301.

35 Wang, Y.; Cao, G. Synthesis and enhanced intercalation properties of nanostructured vanadium oxides. *Chem. Mater.* **2006**, *18*, 2787–2804.

36 Murphy, D. W.; Christian, P. A.; DiSalvo, F. J.; Carides, J. N.; Waszczak, J. V. Lithium incorporation into V_6O_{13} and related vanadium (+4, +5) oxide cathode materials. *J. Electrochem. Soc.* **1981**, *128*, 2053–2060.

37 Li, H.; He, P.; Wang, Y.; Hosono, E.; Zhou, H. High-surface vanadium oxides with large capacities for lithium-ion batteries: from hydrated aerogel to nanocrystalline VO_2(B), V_6O_{13} and V_2O_5. *J. Mater. Chem.* **2011**, *21*, 10999–11009.

38 Hüsing, N.; Schubert, U. Aerogels—airy materials: Chemistry, structure, and properties. *Angew. Chem., Int. Ed.* **1998**, *37*, 22–45.

39 Dong, W.; Rolison, D. R.; Dunn, B. Electrochemical properties of high surface area vanadium oxide aerogels. *Electrochem. Solid-State Lett.* **2000**, *3*, 457–459.

40 Chaput, F.; Dunn, B.; Fuqua, P.; Salloux, K. Synthesis and characterization of vanadium oxide aerogels. *J. Non-Cryst. Solids* **1995**, *188*, 11–18.

41 Le, D. B.; Passerini, S.; Tipton, A. L.; Owens, B. B.; Smyrl, W. H. Aerogels and xerogels of V_2O_5 as intercalation hosts. *J. Electrochem. Soc.* **1995**, *142*, L102–L103.

42 Le, D. B.; Passerini, S.; Guo, J.; Ressler, J.; Owens, B. B.; Smyrl, W. H. High surface area V_2O_5 aerogel intercalation electrodes. *J. Electrochem. Soc.* **1996**, *143*, 2099–2104.

43 Passerini, S.; Le, D. B.; Smyrl, W. H.; Berrettoni, M.; Tossici, R.; Marassi, R.; Giorgetti, M. XAS and electrochemical characterization of lithiated high surface area V_2O_5 aerogels. *Solid State Ionics* **1997**, *104*, 195–204.

44 Mansour, A. N.; Smith, P. H.; Baker, W. M.; Balasubramanian, M.; McBreen, J. In situ XAS investigation of the oxidation state and local structure of vanadium in discharged and charged V_2O_5 aerogel cathodes. *Electrochim. Acta* **2002**, *47*, 3151–3161.

45 Aldebert, P.; Baffier, N.; Gharbi, N.; Livage, J. Layered structure of vanadium pentoxide gels. *Mater. Res. Bull.* **1981**, *16*, 669–676.

46 Guerra, E. M.; Cestarolli, D. T.; Oliveira, H. P. Effect of mesoporosity of vanadium oxide prepared by sol−gel process as cathodic material evaluated by cyclability during Li^+ insertion/deinsertion. *J. Sol−Gel Sci. Technol.* **2010**, *54*, 93–99.

47 Andrukaitis, E.; Bishenden, E. A.; Jacobs, B. W. N.; Lorimer, J. W. Lithium insertion into oriented microcrystals and gels of anhydrous and hydrated vanadium pentoxide. *J. Power Sources* **1989**, *26*, 475–482.

48 Rhodes, C. P.; Dong, W.; Long, J. W.; Rolison, D. R. Controlling defects in nanostructured V_2O_5: Spectroelectrochemical characterization. In *Solid State Ionics VI*; Wachsman, E. D., Swider Lyons, K. E., Carolan, M. F., Garzon, F. H., Liu, M., Stetter, J. R., Eds.; PV 2002−26, Electrochemical Society: Pennington, NJ, 2003; pp 478−489.

49 Passerini, S.; Ressler, J. J.; Le, D. B.; Owens, B. B.; Smyrl, W. H. High rate electrodes of V_2O_5 aerogel. *Electrochim. Acta* **1999**, *44*, 2209–2217.

50 Tang, P. E.; Sakamoto, J. S.; Baudrin, E.; Dunn, B. V_2O_5 aerogel as a versatile host for metal ions. *J. Non-Cryst. Solids* **2004**, *350*, 67–72.

51 Thackeray, M. M.; David, W. I. F.; Goodenough, J. B. Structural characterization of the lithiated iron oxides. *Mater. Res. Bull.* **1982**, *17*, 785–793.

52 Koo, B.; Xiong, H.; Slater, M. D.; Prakapenka, V. B.; Balasubramanian, M.; Podsiadlo, P.; Johnson, C. S.; Rajh, T.; Shevchenko, E. V. Hollow iron oxide nanoparticles for application in lithium-ion batteries. *Nano Lett.* **2012**, *12*, 2429–2435.

53 Quintin, M.; Devos, O.; Delville, M. H.; Campet, G. Study of the lithium insertion−deinsertion mechanism in nanocrystalline γ-Fe_2O_3 electrodes by means of electrochemical impedance spectroscopy. *Electrochim. Acta* **2006**, *51*, 6426–6434.

54 Kanzaki, S.; Inada, T.; Matsumura, T.; Sonoyama, N.; Yamada, A.; Takano, M.; Kanno, R. Nano-sized γ-Fe_2O_3 as lithium battery cathode. *J. Power Sources* **2005**, *146*, 323–326.

55 Kwon, C.-W.; Poquet, A.; Mornet, S.; Campet, G.; Portier, J.; Choy, J.-H. A new polypyrrole/maghemite hybrid as a lithium insertion electrode. *Electrochem. Commun.* **2002**, *4*, 197–200.

56 Bouet, L.; Tailhades, Ph.; Rousset, A.; Domenichini, B.; Gillot, B. Mixed valence states of iron and molybdenum ions in $Mo_xFe_{3-x}O_4$ magnetites and related cation deficient ferrites. *Solid State Ionics* **1992**, *52*, 285–286.

57 Gillot, B.; Nivoix, V. New cation-deficient vanadium-iron spinels with a high vacancy content. *Mater. Res. Bull.* **1999**, *34*, 1735–1747.

58 Bach, S.; Belair, S.; Cachet-Vivier, C.; Pereira-Ramos, J.-P.; Sanchez, L.; Lavela, P.; Tirado, L. Electrochemical proton insertion in $Mn_{2.2}Co_{0.27}O_4$ from aqueous borate solution. *Electrochim. Acta* **1999**, *45*, 931–934.

59 Farcy, J.; Pereira-Ramos, J.-P.; Hernan, L.; Morales, J.; Tirado, J. L. Cation-deficient Mn-Co spinel oxides as electrode material for rechargeable lithium batteries. *Electrochim. Acta* **1994**, *39*, 339–345.

60 Jiménez Mateos, J. M.; Morales, J.; Tirado, J. L. Cation-deficient Mn, Co spinel oxides obtained by thermal decomposition of carbonate precursors. *J. Solid State Chem.* **1989**, *82*, 87–94.

61 Morales, J.; Sánchez, L.; Tirado, J. L. New doped Li-M-Mn-O (M = Al, Fe, Ni) spinels as cathodes for rechargeable 3V lithium batteries. *J. Solid State Electrochem* **1998**, *2*, 420–426.

62 Sánchez, L.; Pereira-Ramos, J.-P. Electrochemical insertion of magnesium in a mixed manganese−cobalt oxide. *J. Mater. Chem.* **1997**, *7*, 471–473.

63 Choi, N. S.; Kim, J. S.; Yin, R. Z.; Kim, S. S. Electrochemical properties of lithium vanadium oxide as an anode material for lithium-ion battery. *Mater. Chem. Phys.* **2009**, *116*, 603–606.

64 Armstrong, A. R.; Lyness, C.; Panchmatia, P. M.; Islam, M. S.; Bruce, P. G. The lithium intercalation process in the low-voltage lithium battery anode $Li_{1+x}V_{1-x}O_2$. *Nat. Mater.* **2011**, *10*, 223–229.

65 Huang, H.; Yin, S.-C.; Nazar, L. F. Approaching theoretical capacity of $LiFePO_4$ at room temperature at high rates. *Electrochem. Solid-State Lett.* **2001**, *4*, A170–A172.

66 Fischer, A. E.; Pettigrew, K. A.; Rolison, D. R.; Stroud, R. M.; Long, J. W. Incorporation of homogeneous, nanoscale MnO_2 within ultraporous carbon structures via self-limiting electrodeposition: Implications for electrochemical capacitors. *Nano Lett.* **2007**, *7*, 281–286.

67 Sassin, M. B.; Mansour, A. N.; Pettigrew, K. A.; Rolison, D. R.; Long, J. W. Electroless deposition of conformal nanoscale iron oxide on carbon nanoarchitectures for electrochemical charge storage. *ACS Nano* **2010**, *4*, 4505–4514.

68 Long, J. W.; Logan, M. S.; Rhodes, C. P.; Carpenter, E. E.; Stroud, R. M.; Rolison, D. R. Nanocrystalline iron oxide aerogels as mesoporous magnetic architectures. *J. Am. Chem. Soc.* **2004**, *126*, 16879–16889.

69 Clauws, P.; Vennik, J. Optical absorption of defects in V_2O_5 single crystals: As-grown and reduced V_2O_5. *Phys. Status Solidi B* **1974**, *66*, 553–560.

70 Rhodes,C. P.; Dong,W.; Long, J. W.; Rolison, D. R. Unpublished data, 2002, U.S. Naval Research Laboratory.